14

Hydrodynamics on Charged Superparamagnetic Microparticles in Water Suspension: Effects of Low-Confinement Conditions and Electrostatics Interactions

P. Domínguez-García[1] and M.A. Rubio[2]

[1]*Dep. Física de Materiales, UNED, Senda del Rey 9, 28040. Madrid*
[2]*Dep. Física Fundamental, UNED, Senda del Rey 9, 28040. Madrid*
Spain

1. Introduction

The study of colloidal dispersions of micro-nano sized particles in a liquid is of great interest for industrial processes and technological applications. The understanding of the microstructure and fundamental properties of this kind of systems at microscopic level is also useful for biological and biomedical applications.

However, a colloidal suspension must be placed somewhere and the dynamics of the micro-particles can be modified as a consequence of the confinement, even if we have a low-confinement system. The hydrodynamics interactions between particles and with the enclosure's wall which contains the suspension are of extraordinary importance to understanding the aggregation, disaggregation, sedimentation or any interaction experienced by the microparticles. Aspects such as corrections of the diffusion coefficients because of a hydrodynamic coupling to the wall must be considered. Moreover, if the particles are electrically charged, new phenomena can appear related to electro-hydrodynamic coupling.

Electro-hydrodynamic effects (Behrens & Grier (2001a;b); Squires & Brenner (2000)) may have a role in the dynamics of confined charged submicron-sized particles. For example, an anomalous attractive interaction has been observed in suspensions of confined charged particles (Grier & Han (2004); Han & Grier (2003); Larsen & Grier (1997)). The possible explanation of this observation could be related with the distribution of surface's charges of the colloidal particles and the wall (Lian & Ma (2008); Odriozola et al. (2006)). This effect could be also related to an electrostatic repulsion with the charged quartz bottom wall or to a spontaneous macroscopic electric field observed on charged colloids (Rasa & Philipse (2004)).

In this work, we are going to describe experiments performed by using magneto-rheological fluids (MRF), which consist (Rabinow (1948)) on suspensions formed by water or some organic solvent and micro or nano-particles that have a magnetic behaviour when a external magnetic field is applied upon them. Then, these particles interact between themselves forming aggregates with a shape of linear chains (Kerr (1990)) aligned in the direction of the magnetic field. When the concentration of particles inside the fluid is high enough, this microscopic behaviour turns to significant macroscopic

consequences, as an one million-fold increase in the viscosity of the fluid, leading to practical and industrial applications, such as mechanical devices of different types (*Lord Corporation, http://www.lord.com/* (n.d.); *N*akano & Koyama (1998); Tao (2000)). This magnetic particle technology has been revealed as useful in other fields such as microfluidics (Egatz-Gómez et al. (2006)) or biomedical techniques (Komeili (2007); Smirnov et al. (2004); Vuppu et al. (2004); Wilhelm, Browaeys, Ponton & Bacri (2003); Wilhelm et al. (2005)).

In our case, we investigate the dynamics of the aggregation of magnetic particles under a constant and uniaxial magnetic field. This is useful not only for the knowledge of aggregation properties in colloidal systems, but also for testing different models in Statistical Mechanics. Using video-microscopy (Crocker & Grier (1996)), we have measured the different exponents which characterize this process during aggregation (Domínguez-García et al. (2007)) and also in disaggregation (Domínguez-García et al. (2011)), i.e., when the chains vanishes as the external field is switched off. These exponents are based on the temporal variation of the aggregates' representative quantities, such as the size s or length l. For instance, the main dynamical exponent z is obtained through the temporal evolution of the chains length $s \sim t^z$. Our experiments analyse the microestructure of the suspensions, the aggregation of the particles under external magnetic fields as well as disaggregation when the field is switched off. The observations provide results that diverge from what a simple theoretical model says. These differences may be related with some kind of electro-hydrodynamical interaction, which has not been taken into account in the theoretical models.

In this chapter, we would like first to summarize the basic theory related with our system of magnetic particles, including magnetic interactions and Brownian movement. Then, hydrodynamic corrections and the Boltzmann sedimentation profile theory in a confined suspension of microparticles will be explained and some fundamentals of electrostatics in colloids are explained. In the next section, we will summarize some of the most recent remarkable studies related with the electrostatic and hydrodynamic effects in colloidal suspensions. Finally, we would like to link our findings and investigations on MRF with the theory and studies explained herein to show how the modelization and theoretical comprehension of these kind of systems is not perfectly understood at the present time.

2. Theory

In this section, we are going to briefly describe the theory related with the main interactions and effects which can be suffered by colloidal magnetic particles: magnetic interactions, Brownian movement, hydrodynamic interactions and finally electrostatic interactions.

2.1 Magnetic particles

By the name of "colloid" we understand a suspension formed by two phases: one is a fluid and another composed of mesoscopic particles. The mesoscopic scale is situated between the tens of nanometers and the tens of micrometers. This is a very interesting scale from a physical point of view, because it is a transition zone between the atomic and molecular scale and the purely macroscopic one.

When the particles have some kind of magnetic property, we are talking about magnetic colloids. From this point of view, two types of magnetic colloids are usually considered: ferromagnetic and magneto-rheologic. The ferromagnetic fluids or ferrofluids (FF) are colloidal suspensions composed by nanometric mono-domain particles in an aqueous or organic solvent, while magneto-rheological fluids (MRF) are suspensions of paramagnetic micro or nanoparticles. The main difference between them is the permanent magnetic moment

of the first type: while in a FF, magnetic aggregation is possible without an external magnetic field, this does not occur in a MRF. The magnetic particles of a MRF are usually composed by a polymeric matrix with small crystals of some magnetic material embedded on it, for example, magnetite. When the particles are superparamagnetic, the quality of the magnetic response is improved because the imanation curve has neither hysteresis nor remanence.
Another point of view for classifying these suspensions is the rheological perspective. By rheology, we name the discipline which study deformations and flowing of materials when some stress is applied. In some ranges, it is possible to consider the magnetic colloids as Newtonian fluids because, when an external magnetic field is applied, the stress is proportional to the velocity of the deformation. On a more global perspective, these fluids can be immersed on the category of complex fluids (Larson (1999)) and are studied as complex systems (Science. (1999)).
Now we are going to briefly provide some details about magnetic interactions: magnetic dipolar interaction, interaction between chains and irreversible aggregation.

2.1.1 Magnetic dipolar interaction

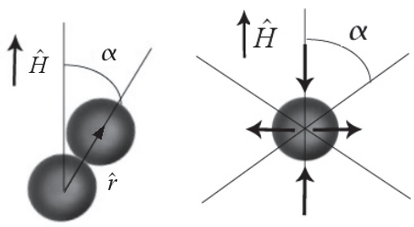

Fig. 1. Left: Two magnetic particles under a magnetic field $\vec{H}$. The angle between the field direction and the line that join the centres of the particles is named as α. Right: The attraction cone of a magnetic particle. Top and bottom zones are magnetically attractive, while regions on the left and on the right have repulsive behaviour.

As it has been said before, the main interest of MRF are their properties in response to external magnetic fields. These properties can be optical (birefringence (Bacri et al. (1993)), dichroism (Melle (2002))) or magnetical or rheological. Under the action of an external magnetic field, the particles acquire a magnetic moment and the interaction between the magnetic moments generates the particles aggregation in the form of chain-like structures. More in detail, when a magnetic field $\vec{H}$ is applied, the particles in suspension acquire a dipolar moment:

$$\vec{m} = \frac{4\pi a^3}{3}\vec{M} \tag{1}$$

where $\vec{M} = \chi\vec{H}$ and a are respectively the particle's imanation and radius, whereas χ is the magnetic susceptibility of the particle.
The most simple way for analysing the magnetic interaction between magnetic particles is through the dipolar approximation. Therefore, the interaction energy between two magnetic dipoles $\vec{m}_i$ and $\vec{m}_j$ is:

$$U_{ij}^d = \frac{\mu_0\mu_s}{4\pi r^3}\left[(\vec{m}_i\cdot\vec{m}_j) - 3(\vec{m}_i\cdot\hat{r})(\vec{m}_j\cdot\hat{r})\right] \tag{2}$$

where $\vec{r}_i$ is the position vector of the particle i, $\vec{r} = \vec{r}_j - \vec{r}_i$ joins the centre of both particles and $\hat{r} = \vec{r}/r$ is its unitary vector.

Then, we can obtain the force generated by $\vec{m}_i$ under $\vec{m}_j$ as:

$$\vec{F}_{ij}^{d} = \frac{3\mu_0\mu_s}{4\pi r^4}\left\{\left[(\vec{m}_i\cdot\vec{m}_j) - 5(\vec{m}_i\cdot\hat{r})(\vec{m}_j\cdot\hat{r})\right]\hat{r} + (\vec{m}_j\cdot\hat{r})\vec{m}_i + (\vec{m}_i\cdot\hat{r})\vec{m}_j\right\} \tag{3}$$

If both particles have identical magnetic properties and knowing that the dipole moment aligns with the field, we obtain the following two expressions for potential energy and force:

$$U_{ij}^{d} = \frac{\mu_0\mu_s m^2}{4\pi r^3}(1-3\cos^2\alpha) \tag{4}$$

$$\vec{F}_{ij}^{d} = \frac{3\mu_0\mu_s m^2}{4\pi r^4}\left[(1-3\cos^2\alpha)\hat{r} - \sin(2\alpha)\hat{\alpha}\right] \tag{5}$$

where α is the angle between the direction of the magnetic field $\hat{H}$, and the direction set by $\hat{r}$ and where $\hat{\alpha}$ is its unitary vector.
From the above equations, it follows that the radial component of the magnetic force is attractive when $\alpha < \alpha_c$ and repulsive when $\alpha > \alpha_c$, where $\alpha_c = \arccos\frac{1}{\sqrt{3}} \simeq 55^\circ$, so that the dipolar interaction defines an hourglass-shaped region of attraction-repulsion in the complementary region (see Fig.1). In addition, the angular component of the dipolar interaction always tends to align the particles in the direction of the applied magnetic field. Thus, the result of this interaction will be an aggregation of particles in linear structures oriented in the direction of $\hat{H}$.
The situation depicted here is very simplified, especially from the viewpoint of magnetic interaction itself. In the above, we have omitted any deviations from this ideal behaviour, such as multipole interactions or local field (Martin & Anderson (1996)). Multipolar interactions can become important when $\mu_p/\mu_s \gg 1$. The local field correction due to the magnetic particles themselves generate magnetic fields that act on other particles, increasing the magnetic interaction. For example, when the magnetic susceptibility is approximately $\chi \sim 1$, this interaction tends to increase the angle of the cone of attraction from 55° to about 58° and also the attractive radial force in a 25% and the azimuth in a 5% (Melle (2002)).
One type of fluid, called electro-rheological (ER fluids) is the electrical analogue of MRF. This type of fluid is very common in the study of kinematics of aggregation. Basically, the ER fluids consist of suspensions of dielectric particles of sizes on the order of micrometers (up to hundreds of microns) in conductive liquids. This type of fluid has some substantial differences with MRF, especially in view of the ease of use. The development of devices using electric fields is more complicated, requiring high power voltage; in addition, ER fluids have many more problems with surface charges than MRF, which must be minimized as much as possible in aggregation studies. However, basic physics, described above, are very similar in both systems, due to similarities between the magnetic and electrical dipolar interaction.

2.1.2 Magnetic interaction between chains

Chains of magnetic particles, once formed, interact with other chains in the fluid and with single particles. In fact, the chains may laterally coalesce to form thicker strings (sometimes called columns). This interaction is very important, especially when the concentration of particles in suspension is high. The first works that studied the interaction between chains of particles come from the earliest studies of external field-induced aggregation (Fermigier & Gast (1992); Fraden et al. (1989))

Basically, the aggregation process has two stages: first, the chains are formed on the basis of the aggregation of free particles, after that, more complex structures are formed when chains aggregate by lateral interaction. When the applied field is high and the concentration of particles in the fluid is low, the interactions between the chains are of short range. Under this situation, there are two regions of interaction between the chains depending on the lateral distance between them: when the distance between two strings is greater than two diameters of the particle, the force is repulsive; if the distance is lower, the resultant force is attractive, provided that one of the chains is moved from the other a distance equal to one particle's radius in the direction of external field (Furst & Gast (2000)). In this type of interactions, the temperature fluctuations and the defects in the chains morphology are particularly important. Indeed, variations on these two aspects generate different types of theoretical models for the interaction between chains. The model that takes into account the thermal fluctuations in the structure of the chain for electro-rheological fluids is called *HT* (Halsey & Toor (1990)), and was subsequently extended to a modified HT model (MHT) (Martin et al. (1992)) to include dependence on field strength. The latter model shows that only lateral interaction occurs between the chains when the characteristic time associated with their thermal relaxation is greater than the characteristic time of lateral assembling between them. Possible defects in the chains can vary the lateral interaction, mainly through perturbations in the local field.

2.1.3 Irreversible aggregation

The irreversible aggregation of colloidal particles is a phenomenon of fundamental importance in colloid science and its applications. Basically, there are two basic scenarios of irreversible colloidal aggregation. The first, exemplified by the model of Witten & Sander (1981), is often referred to as Diffusion-Limited Aggregation (DLA). In this model, the particles diffuse without interaction between them, so that aggregation occurs when they collide with the central cluster. The second scenario is when there is a potential barrier between the particles and the aggregate, so that aggregation is determined by the rate at which the particles manage to overcome this barrier. The second model is called Colloid Reaction-Limited Aggregation (RLCA). These two processes have been observed experimentally in colloidal science (Lin et al. (1989); Tirado-Miranda (2001)).

These aggregation processes are often referred as fractal growth (Vicsek (1992)) and the aggregates formed in each process are characterized by a concrete fractal dimension. For example, in DLA we have aggregates with fractal dimension $D_f \sim 1.7$, while RLCA provides $D_f \sim 2.1$. A very important property of these systems is precisely that its basic physics is independent of the chemical peculiarities of each system colloidal i.e., these systems have universal aggregation. Lin et al. (1989) showed the universality of the irreversible aggregation systems performing light scattering experiments with different types of colloidal particles and changing the electrostatic forces in order to study the RLCA and DLA regimes in a differentiated way. They obtained, for example, that the effective diffusion coefficient (Eq.28) did not depend on the type of particle or colloid, but whether the process aggregation was DLA or RLCA.

The DLA model was generalized independently by Meakin (1983) and Kolb et al. (1983), allowing not only the diffusion of particles, but also of the clusters. In this model, named Cluster-Cluster Aggregation (CCA), the clusters can be added by diffusion with other clusters or single particles. Within these systems, if the particles are linked in a first touch, we obtain the DCLA model. The theoretical way to study these systems is to use the theory of von Smoluchowski (von Smoluchowski (1917)) for cluster-cluster aggregation among Monte Carlo

simulations (Vicsek (1992)). This theory considers that the aggregation kinetics of a system of N particles, initially separated and identical, aggregate; and these clusters join themselves to form larger objects. This process is studied through the distribution of cluster sizes $n_s(t)$ which can be defined as the number of aggregates of size s per unit of volume in the system at a time t. Then, the temporal evolution is given by the following set of equations:

$$\frac{dn_s(t)}{dt} = \frac{1}{2}\sum_{i+j=s} K_{ij} n_i n_j - n_s \sum_{j=1} K_{sj} n_j, \tag{6}$$

where the kernel K_{ij} represents the rate at which the clusters of size i and j are joined to form a cluster of size $s = i + j$. All details of the physical system are contained in the kernel K_{ij}, so that, for example, in the DLA model, the kernel is proportional to the product of the cross-section of the cluster and the diffusion coefficient. Eq.6 has certain limitations because only allows binary aggregation processes, so it is just applied to processes with very low concentration of particles.

A scaling relationship for the cluster size distribution function in the DCLA model was introduced by Vicsek & Family (1984) to describe the results of Monte Carlo simulations. This scaling relationship can be written as:

$$n_s \sim s^{-2} g\left(s/S(t)\right) \tag{7}$$

where $S(t)$ is the average cluster size of the aggregates:

$$S(t) \equiv \frac{\sum_s s^2 n_s(t)}{\sum_s s n_s(t)} \tag{8}$$

and where the function $g(x)$ is in the form:

$$g(x) \begin{cases} \sim x^{\Delta} \text{ if } x \ll 1 \\ \ll 1 \text{ if } x \gg 1 \end{cases}$$

One consequence of the scaling 7 is that a temporal power law for the average cluster size can be deduced:

$$S(t) \sim t^{z} \tag{9}$$

Calculating experimentally the average cluster size along time, we can obtain the kinetic exponent z. Similarly to $S(t)$ is possible to define an average length in number of aggregates $l(t)$:

$$l(t) \equiv \frac{\sum_s s\, n_s(t)}{\sum_s n_s(t)} = \frac{1}{N(t)} \sum_s s\, n_s(t) = \frac{N_p}{N(t)} \tag{10}$$

where $N(t) = \sum n_s(t)$ is the total number of cluster in the system at time t and $N_p = \sum s\, n_s(t)$ is the total number of particles. Then, it is expected that N had a power law form with exponent z':

$$N(t) \sim t^{-z'} \tag{11}$$

$$l(t) \sim t^{z'} \tag{12}$$

2.2 Brownian movement and microrheology

Robert Brown[1] (1773-1858) discovered the phenomena that was denoted with his name in 1827, when he studied the movement of pollen in water. The explanation of Albert Einstein in 1905 includes the named Stokes-Einstein relationship for the diffusion coefficient of a particle of radius a immersed in a fluid of viscosity η at temperature T:

$$D = \frac{k_B T}{6\pi a \eta} \tag{13}$$

where k_B is the Boltzmann constant. This equation can be generalized for an object (an aggregate) formed by a number of particles N:

$$D = \frac{k_B T}{6\pi \eta R_g}$$

where R_g is the radius of gyration defined as $R_g(N) = \sqrt{1/N \sum_{i=1}^{N} r_i^2}$, where r_i is the distance between the i particle to the centre of mass of the cluster. If $R_g = a$, we recover the Stokes-Einstein expression.

Let's see how to calculate the diffusion coefficient D from the observation of individual particles moving in the fluid. The diffusion equation says that:

$$\frac{\partial \rho}{\partial t} = D\nabla^2 \rho$$

where ρ is here the probability density function of a particle that spreads a distance Δr at time t. This equation has as a solution:

$$\rho(\Delta r, t) = \frac{1}{(4\pi D t)^{3/2}} e^{-\Delta r^2/4Dt} \tag{14}$$

If the Brownian particle moves a distance Δr in the medium on which is immersed after a time δt, then the mean square displacement (MSD) weighted with the probability function given by Eq.14 is given by:

$$\left\langle (\Delta r)^2 \right\rangle = \left\langle |r(t+\delta t) - r(t)|^2 \right\rangle = 6Dt \tag{15}$$

The diffusion coefficient can be obtained by 15 and observing the displacement Δr of the particle for a fixed δt. In two dimensions, the equations 14 and 15 are:

$$\rho(\Delta r, t) = \frac{1}{(4\pi D t)} e^{-\Delta r^2/4Dt} \tag{16}$$

$$\left\langle |r(t+\delta t) - r(t)|^2 \right\rangle = 4Dt \tag{17}$$

The equations 13 and 15 are the basis for the development of a experimental technique known as microrheology (Mason & Weitz (1995)). This technique consists of measuring viscosity and other mechanical quantities in a fluid by monitoring, using video-microscopy, the movement

[1] Literally: *While examining the form of these particles immersed in water, I observed many of them very evidently in motion [..]. These motions were such as to satisfy me, after frequently repeated observation, that they arose neither from currents in the fluid, nor from its gradual evaporation, but belonged to the particle itself.* (Edinburgh New Philosophical Journal, Vol. 5, April to September, 1828, pp. 358-371)

of micro-nano particles (regardless their poralization). Thus, it is possible to obtain the viscosity of the medium simply by studying the displacement of the particle in the fluid. The microrheology has been widely used since the late nineties of last century (Waigh (2005)). Due to microrheology needs and for the sake of the analysis of the thermal fluctuation spectrum of probe spheres in suspension, the generalized Stokes-Einstein equation (Mason & Weitz (1995)) was developed. This expression is similar to Eq.13, but introducing Laplace transformed quantities:

$$\tilde{D}(s) = \frac{k_B\, T}{6\pi a s\, \tilde{\eta}_s} \tag{18}$$

where s is the Laplace frequency, and $\tilde{\eta}_s$ and $\tilde{D}(s)$ are the Laplace transformed viscosity and diffusion coefficient. The dynamics of the Brownian particles can be very different depending on the mechanical properties of the fluid. This equation is the base for the rheological study, by obtaining its viscoelastic moduli (Mason (2000)), of the complex fluid in which the particles are immersed.

If we only track the random motion of colloidal spheres moving freely in the fluid, we are talking of "passive" microrheology, but there are variations on this technique named "active" microrheology, for example, using optical tweezers (Grier (2003)). This technique allows to study the response of colloidal particles in viscoelastic fluids and the structure of fluids in the micro-nanometer scales (Furst (2005)), measure viscoelastic properties of biopolymers (like DNA) and the cell membrane (Verdier (2003)). Other useful methodologies are the two-particles microrheology (Crocker et al. (2000)) which allows to accurately measure rheological properties of complex materials, the use of rotating chains following an external rotating magnetic field (Wilhelm, Browaeys, Ponton & Bacri (2003); Wilhelm, Gazeau & Bacri (2003)) or magnetic bead microrheometry (Keller et al. (2001)).

2.3 Hydrodynamics

When we are talking about hydrodynamics in a colloidal suspension of particles we need to introduce the Reynolds number, Re, defined as:

$$\mathrm{Re} \equiv \frac{\rho_r\, v\, a}{\eta} \tag{19}$$

where ρ_r is the relative density, a is the particle radius, v is the velocity of the particle in the fluid which has a viscosity η. This number reflects the relation between the inertial forces and the viscous friction. If we are in a situation of low Reynolds number dynamics, as it usually happens in the physical situation here studied, the inertial terms in the Newton equations can be neglected, and $m\ddot{x} \cong 0$.

However, even in the case of low Reynolds number, the diffusion coefficient of particles in a colloidal system may have certain deviations from the expressions explained above. The diffusion coefficient can vary due to hydrodynamic interactions between particles, the morphology of the clusters, or because of the enclosure containing the suspension. When a particle moves near a "wall", the change in the Brownian dynamics of the particle is remarkable. The effective diffusion coefficient then varies with the distance of the particle from the wall (Russel et al. (1989)), the closer is the particle to the wall, the lower the diffusion coefficient. The interest of the modification on Brownian dynamics in confinement situations is quite large, for example to understand how particles migrate in porous media, how the macromolecules spread in membranes, or how cells interact with surfaces.

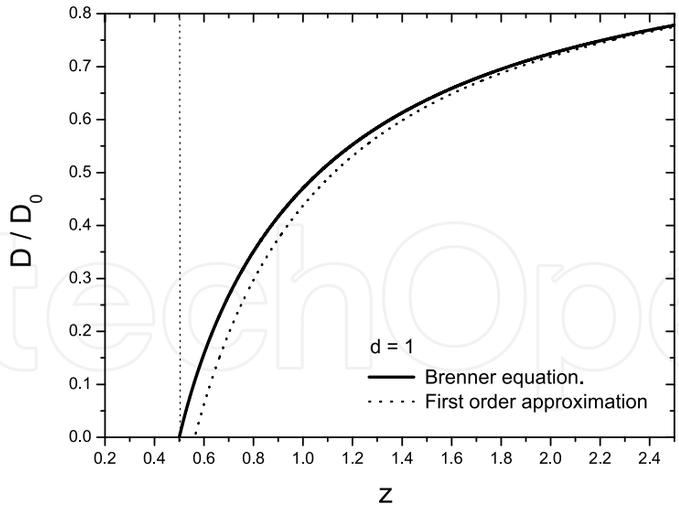

Fig. 2. Comparative analysis between the relative diffusion coefficient for the Brenner equation (Eq.20) and the first order approximation (Eq.21), as a function of the distance to the wall z for a particle of diameter 1 (z-unit are in divided by the diameter of the particle). These two expressions are practically equal when $z \geq 1.5$.

2.3.1 Particle-wall interaction

When a particle diffuses near a wall, thanks to the linearity of Stokes equations, the diffusion coefficient can be separated into two components, one parallel to the wall $D_{\shortparallel}$ and the other perpendicular $D_{\perp}$. In the literature, several studies in this regard can be found (Crocker (1997); Lin et al. (2000); Russel et al. (1989)). One particularly important is the study of Faucheux & Libchaber (1994) where measurements of particles confined between two walls are reported. This work provides a table with the diffusion coefficients obtained (theoretical and experimental) for different samples (different radius and particles) and different distances from the wall, from 1 to 12 μm. For example, for a particle diameter 2.5 μm, a distance of 1.3 μ m from the wall and with a density 2.1 times that of water, a diffusion coefficient $D/D_0 = 0.32$ is obtained, where D_0 is the diffusion coefficient given by Eq.13.

There are no closed analytical solutions for this type of problem, with the exception of that obtained for a sphere moving near a flat wall in the direction perpendicular to it (Brenner (1961)):

$$\frac{D_{\perp}(z)}{D_0} = \left\{ \frac{4}{3}\sinh\alpha \sum_{n=1}^{\infty} \frac{n(n+1)}{(2n-1)(2n+3)} \left[\frac{2\sinh[(2n+1)\alpha] + (2n+1)\sinh[2\alpha]}{4\sinh^2[(n+1/2)\alpha] - (2n+1)^2\sinh^2[\alpha]} - 1 \right] \right\}^{-1} \tag{20}$$

where $\alpha \equiv \operatorname{arccosh}(z/a)$ and a is the radius particle and z is the distance between the centre of the particle and the wall.

Theoretical calculations in this regard are generally based on the methods of reflections, which involves splitting the hydrodynamic interaction between the wall and the particle in a linear superposition of interactions of increasing order. Using this method, it is possible to obtain a iterative solution for this problem in power series of (a/z). In the case of the perpendicular direction it is found:

$$\frac{D_{\perp}(z)}{D_0} \cong 1 - \frac{9}{8}\left(\frac{a}{z}\right) + O\left(\frac{a}{z}\right)^3 \tag{21}$$

In the Fig.2 a comparison between the exact equation 20 and this first order expression 21 is plotted. These two expressions provide similar results when $z \geq 1.5$.
In the case of the parallel direction to the wall we have the following approximation :

$$\frac{D_{\shortparallel}(z)}{D_0} \cong 1 - \frac{9}{16}\frac{a}{z} + \frac{1}{8}\frac{a^3}{z^3} - \frac{45}{256}\frac{a^4}{z^4} - \frac{1}{16}\frac{a^5}{z^5} + ... \tag{22}$$

which is commonly used in their first order:

$$\frac{D_{\shortparallel}(z)}{D_0} \cong 1 - \frac{9}{16}\left(\frac{a}{z}\right) + O\left(\frac{a}{z}\right)^3 \tag{23}$$

If we are thinking about one particle between two close walls, Dufresne et al. (2001) showed how it is possible to deduce, using the Stokeslet method (Liron & Mochon (1976)), a very complicated closed expression for the diffusion coefficients when $a \ll h$, being h the distance between the two walls. However, the method of reflections gives approximated theoretical expressions. Basically, there are three approximations that provide good results and which are different because of small modifications in the drag force. The first of these methods is the Linear Superposition Approximation (LSA) where the drag force over the sphere is chosen as the sum of the force that makes all the free fluid over the sphere. A second method is the Coherent Superposition Approximation (CSA) whose modification proposed by Bensech & Yiacoumi (2003) was named as Modified Coherent Superposition Approximation (MCSA) and gives the following expression:

$$\frac{D(z)}{D_0} = \left\{ 1 + [C(z) - 1] + [C(h - z) - 1] + \sum_{n=1}^{\infty} (-1)^n \frac{nh - z - a}{nh - z} [C(nh + z) - 1] \right.$$
$$\left. + \sum_{n=1}^{\infty} (-1)^n \frac{(n-1)h + z - a}{(n-1)h + z} [C((n+1)h - z) - 1] \right\}^{-1} \tag{24}$$

where the function $C(z)$ is the inverse of the normalized diffusion coefficient ($D_0/D(z)$) in the only one wall situation.
Another interesting physical configuration is the hydrodynamic coupling of two Brownian spheres near to a wall. Dufresne et al. (2000) showed that the collective diffusion coefficients in the directions parallel and perpendicular to the surface are related by a hydrodynamical coupling because of the fact that the surrounded fluid moved by one of the particles affects the other. This wall-induced effect may have an influence in the origin of some anomalous effects in experiments of confined microparticles in suspension.

2.3.2 Particle-particle interaction

Another effect of considerable importance, or at least, that we must take into account, is the hydrodynamic interaction between two particles. This effect is quantified by the parameter $\rho = r/a$ where r is the radial distance between the centres of the particles and a is their radius. Crocker (1997) showed how the modification of the diffusion coefficient due to the mutual hydrodynamic interaction between the two particles varies in the directions parallel or perpendicular to the line joining the centres of mass. Finally, they obtained that the predominant effect is the one that occurs in the radial direction and which is given by:

$$\frac{D}{D_0} \cong -\frac{15}{4\rho^4} \tag{25}$$

The effect in the perpendicular direction is much lower and negligible ($O(\rho^{-6})$).

2.3.3 Anisotropic friction

When the aggregates are formed in the suspensions, their way of spreading in the fluid is expected to change. By analogy with the Stokes-Einstein equation, in which the diffusion coefficient depends on the inverse of particle diameter ($D \sim a^{-1}$), Miyazima et al. (1987) suggested that the diffusion coefficient depends on the inverse cluster size s in the form $D(s) \sim s^{\gamma}$, where γ is the coefficient that marks the degree of homogeneity of the kernel on the Smoluchowski equation (Eq. 6). The result for the diffusion coefficient $\gamma = -1$ is considered to be strictly valid for spherical particles that not interact hydrodynamically among them. However, in the case of an anisotropic system, as is the case of chain aggregates, the diffusion coefficient varies due to the hydrodynamic interaction in the direction parallel and perpendicular to the axis of the chain, as follows (Doi & Edwards (1986)):

$$D_{\shortparallel} = \frac{k_B T}{2\pi\eta a}\frac{\ln s}{s} \tag{26}$$

$$D_{\perp} = D_{\shortparallel}/2 \tag{27}$$

This result is based assuming point particles, but similar expressions are obtained by modelling the aggregates in the form of cylinders of length L and diameter $d = 2a$. Tirado & García (1979; 1980) provide diffusion coefficients for this objects in the directions perpendicular, parallel and rotational to the axis of the chains ($D_{\shortparallel}, D_{\perp}, D_r$).
By using mesaurements of Dynamic Light Scattering (DLS), an effective diffusion coefficient, D_{eff}, of the aggregates can be extracted (Koppel (1972)). This effective coefficient is related to the others mentioned above by means of the relationship:

$$D_{\text{eff}} = D_{\perp} + \frac{L^2}{12}D_r \tag{28}$$

which is correct if $qL >> 1$ where q is the scattering wave vector defined as: $q = 4\pi/\lambda_l \sin(\theta/2)$, λ_l is the wave length of the laser over the suspension and θ is the scattering angle.

2.3.4 Cluster sedimentation

A particularly important effect is the sedimentation of the clusters or aggregates. It is essential, when a colloidal system is studied, determine the position of the aggregates from the wall, as well as knowing what the deposition rate by gravity is and when the equilibrium in a given layer of fluid is reached. The velocity v_c experienced by a cluster composed of N identical spherical particles of radius a and mass M falling by gravity in a fluid without the presence of walls is (González et al. (2004)):

$$v_c = \frac{MgN}{\gamma_0}\left(1 - \frac{\rho}{\rho_p}\right) = \frac{MgDN}{k_B T}\left(1 - \frac{\rho}{\rho_p}\right)$$

where g is the value of the gravity acceleration, ρ is the fluid density, ρ_p is the density of the particles, γ_0 is t the drag coefficient and D the diffusion coefficient. If we have only one spheric particle, the last equation yields the classic result for the sedimentation velocity:

$$v_p = \frac{2a^2 g\Delta\rho}{9\eta}$$

with $\Delta\rho = \rho_p - \rho$. We can define the Péclet number as the ratio between the sedimentation time t_s and diffusion t_d using a fixed distance, for instance, $2a$:

$$P_e \equiv \frac{t_d}{t_s} = \frac{Mga}{k_B T}\left(1 - \frac{\rho}{\rho_p}\right) = \frac{4\pi a^4 g \Delta\rho}{3k_B T} \tag{29}$$

Then, the vertical distance travelled by gravity for a cluster in a time equal to that a particle spread a distance equal to the diameter of the particle d is $d_c = v_c t_d = P_e N d$.
The above expressions are satisfied when sedimentation occurs in an unconfined fluid. If there is a bottom wall, then it provides a spatial distribution of particles ρ which depends on the relative height with respect to the bottom wall. If the system is in an equilibrium state and with low concentration of particles, we can use the Boltzmann density profile, which measures the balance on the thermal forces and gravity:

$$\ln \rho(z) \propto -\frac{z}{L_G} \tag{30}$$

where $L_G \sim k_B T/Mg$. As mentioned, this density profile is valid when the interactions between the colloidal particles are neglected. However, experimental situations can be much more complicated, resulting in deviations from this profile, so theoretical research is still in development about this question (Chen & Ma (2006); Schmidt et al. (2004)). In fact, it has been discovered experimentally that the influence of the electric charge of silica nanoparticles in a suspension of ethanol may drastically change the shape of the density profile (Rasa & Philipse (2004)). We will here assume the expression 30 to be correct, so that the average height z_m of a particle of radius a, between two walls separated by a distance h, can be determined by the Boltzmann profile as Faucheux & Libchaber (1994) showed:

$$P_B(z) = \frac{1}{L}\left(\frac{e^{-z/L}}{e^{-a/L} - e^{(a-h)/L}}\right) \tag{31}$$

where z is the position of the particle between the two walls, where the bottom wall is at $z = 0$ and the top is located at $z = h$, L is the characteristic Boltzmann length defined as $L \equiv k_B T\,(g\Delta M)^{-1}$ where $\Delta M \equiv (4/3)\pi a^3(\rho_p - \rho)$.
Therefore, the mean distance z_m can be calculated:

$$\begin{aligned} z_m &= \int_a^{h-a} z P_B(z) dz = \\ &= \frac{e^{-a/L}[aL + L^2] - e^{(a-h)/L}[(h-a)L + L^2]}{L[e^{-a/L} - e^{(a-h)/L})} \end{aligned} \tag{32}$$

With that expression and the equations for the diffusion coefficient near a wall (Eqs. 20 to 25) we can estimate the effective diffusion coefficient of a sedimented particle. However, when we have a set of particles, clusters or aggregates near the walls of the enclosure, the evaluation of hydrodynamic effects on the diffusion coefficient and their dynamics is not an easy problem to evaluate theoretically or experimentally. In fact, this problem is very topical, for example, focused on polymer science (Hernández-Ortiz et al. (2006)) or more specifically, in the case of biopolymers, such as DNA strands, moving by low flows in confined enclosures (Jendrejack et al. (2003)). Kutthe (2003) performed Stokestian dynamics simulations (SD) of chains, clusters and aggregates in various situations in which hydrodynamic interactions

are not negligible. Specifically, they calculated the friction coefficient γ_N depending on N (number of particles) for linear chains located at a distance z of the wall and applying a transverse velocity $V_x = 0.08$ diameters per second. The friction coefficient γ_N, to reach a velocity V_x in the transverse direction was obtained as:

$$\gamma_N = \frac{F_x}{3\pi\eta d V_x}$$

where F_x is the force over the chain and d the diameter of the particle. Then, they obtain that, far away from the wall, $\gamma_{30} \sim 6$ for a chain formed by 30 particles. But, near enough from the wall, the friction coefficient grows to a value $\gamma_{30} \sim 200$. Recently, Paddinga & Briels (2010) showed simulation results for translational and rotational friction components of a colloidal rod near to a planar hard wall. They obtained a enhancement friction tensor components because of the hydrodynamic interactions between the rod and the wall.
In any case, when we are thinking on one spherical Brownian particle, we can estimate the diffusion coefficient using the Boltzmann profile by calculating the mean position of the particle using Eq.32. Then, if we can calculate the experimental diffusion coefficient when sedimentation affects to the particles, we can employ the following expression (Domínguez-García, Pastor, Melle & Rubio (2009); Faucheux & Libchaber (1994)):

$$D_{||}^{\delta} = \int_0^L P_B(z) \left[\int_{z-\delta(z,\eta)}^{z+\delta(z,\eta)} D_{||}(z',\eta) \frac{P_B(z')}{N_B(z',\eta)} dz' \right] dz$$

where $P_B(z)$ is the Boltzmann probability distribution, $N_B(z)$ is the normalization of that function, $D_{||}(z',\eta)$ is the corrected diffusion coefficient of the particle for the motion parallel to the wall. This expression introduces a correction because of the vertical movement: during each time window of span τ, the particle typically explores a region of size 2δ with $\delta(z,\eta) = \frac{1}{2}\sqrt{2\tau D_{\perp}(z,\eta)}$, where $D_{\perp}$ is the diffusion coefficient for the motion normal to the wall. The height of the particle from the bottom, z, is calculated by assuming the Boltzmann probability distribution.

2.4 Electrostatics

In a colloidal system, there are usually present not only external forces or hydrodynamic interaction of particles with the fluid, but also electrostatic interactions of various kinds. Moreover, as we shall see, many of the commercial micro-particles have carboxylic groups ($-COOH$) to facilitate their possible use, for example, in biological applications. These groups provide for electrolytic dissociation, a negative charge on the particle surface, so that we can see their migration under a constant and uniaxial electric field using the technique of electrophoresis. Therefore, these groups generate an electrostatic interaction between the particles.

2.4.1 DLVO theory

DLVO theory (Derjaguin & Landau (1941); Verwey & Overbeek (1948)) is the commonly used classical theory to explain the phenomena of aggregation and coagulation in colloidal particle systems without external fields applied. Roughly speaking, the theory considers that the colloidal particles are subject to two types of electrical forces: repulsive electrostatic forces due to same-sign charged particles and, on the other hand, Van der Waals forces which are of attractive nature and appear due to the interaction between the molecules that form the colloid. According to the intensity relative to each other, the particles will aggregate or repel.

Thus, the method to control the aggregation is to vary the ionic strength of medium, i.e., the pH. In most applications in colloids, it is enormously important to control aggregation of particles, for example, for purification treatments of water.
The situation around a negatively charged colloidal particle is approximately described by the double layer model. This model is used to display the ionic atmosphere in the vicinity of the charged colloid and explain how the repulsive electrical forces act. Around the particle, the negative charge forms a rigid layer of positive ions from the fluid, usually called Stern layer. This layer is surrounded by the diffuse layer that is formed by positive ions seeking to approach the colloidal particle and that are rejected by the Stern layer. In the diffuse layer there is a deficit of negative ions and its concentration increases as we left the colloidal particle. Therefore, the diffuse layer can be viewed as a positively charged atmosphere surrounding the colloid.
The two layers, the Stern layer and diffuse layer, form the so-called double layer. Therefore, the negative particle and its atmosphere produce a positive electrical potential associated with the solution. The potential has its maximum value on the surface of the particle and gradually decreases along the diffuse layer. The value of the potential that brings together the Stern layer and the diffuse layer is known as the Zeta potential, whose interest mainly lies in the fact that it can be measured. This Zeta potential measurement, is commonly referred as ζ and measured in mV. The Zeta potential is usually measured using the Laser Doppler Velocimeter technique. This device applies an electric field of known intensity of the suspension, while this is illuminated with a laser beam. The device measures the rate at which particles move so that the Zeta potential, ζ, can be calculated by several equations that relate the Zeta potential electrophoretic mobility, μ_e.
In a general way, it is possible to use the following expression, known as the Hückel equation:

$$\mu_e = \frac{2}{3}\frac{\varepsilon\zeta}{\eta} f(\kappa a) \tag{33}$$

where ε is the dielectric constant of the medium, η its viscosity, a the radius of the particle and where $1/\kappa$ is the width of the double layer, known as the Debye screening length and where $f(\kappa a)$ is the named Henry function. In the case of $1 < \kappa a < 100$, the Zeta potentials can be calculated by means of some analytic expression of the Henry function (Otterstedt & Brandreth. (1998)). Summarising, the higher is the Zeta potential, the more intense will be the Coulombian repulsion between the particles and the lower will be the influence of the Van der Waals force in the colloid.
The Van der Walls potential, which can provide a strong attractive interaction, is usually neglected because its influence is limited to very short surface-to-surface distances in the order of 1 nm. Therefore, the DLVO electrostatic potential between two particles located a radial distance r one from the other is usually given by the classical expression:

$$U(r) = \frac{(Z^* e)^2}{\varepsilon}\frac{\exp(2a\kappa)}{(1+a\kappa)^2}\frac{\exp(-\kappa r)}{r} \tag{34}$$

where Z^* is the effective charge of the particles and $\sigma_{\text{eff}} = Z^* e/4\pi a^2$ is their density of effective charge. Therefore, in this theory, two spherical like-charged colloidal particles suffered a purely electrostatic repulsion between them. The colloidal particle can have carboxylic groups ($COOH$) attached to their surfaces, creating a layer of negative charge of length δ in the order of nanometers surrounding the colloidal particles (Shen et al. (2001)).

The presence of this layer modifies the equation of the double-layer potential (Reiner & Radke (1993); Shen et al. (2001)):

$$U_{dl}(s) = 2\pi\varepsilon(\psi)^2 \frac{2}{2 + s'/a} \exp(-\kappa s') \tag{35}$$

where $s' = s - 2\delta$.

2.4.2 Ornstein-Zernike equation

For calculating the electrostatic potential in a colloidal suspension, we can use the following methodology. This approach involves using the radial distribution function of the particles, $g(r)$, knowing that it is related with the interaction energy of two particles in the limit of infinite dilution by means of the Boltzmann distribution:

$$\lim_{n \to 0} g(r) = e^{-\beta U(r)} \tag{36}$$

where n is the particle density and $\beta \equiv 1/k_B T$. However, for finite concentrations, $g(r)$ is influenced by the proximity between particles, so we can calculate the mean force potential, $w(r)$:

$$w(r) = -\frac{1}{\beta} \ln g(r) \tag{37}$$

But we do not know the relation between $w(r)$ and $U(r)$. Here, is usually defined a total correlation function $h(r) \equiv g(r) - 1$ and is used the Ornstein-Zernike (O-Z) equation for two particles in a two-dimensional fluid:

$$h(r) = c(r) + n \int c(r') h(|\mathbf{r}' - \mathbf{r}|) dr' \tag{38}$$

The $c(r)$ function is the direct correlation function between two particles. Now, it is necessary to close the integral equation by linking $h(r)$, $c(r)$ and $U(r)$. For that, one of the following assumptions is employed:

$$c(r) = \begin{cases} -\beta U(r) & \text{MSA} \\ -\beta U(r) + h(r) - \ln g(r) & \text{HNC} \\ (1 - e^{\beta U})(1 + h(r)) & \text{PY} \end{cases} \tag{39}$$

named Mean Spherical Approximation (MSA), Hypernetted Chain (HNC) and Percus-Yevick (PY).

In the case of video-microscopy experiments, a more practical methodology is explained by Behrens & Grier (2001b) for obtaining the electrostatic potential. More explicitly, with the PY approximation we have:

$$U(r) = w(r) + \frac{n}{\beta} I(r) = -\frac{1}{\beta} \left[\ln g(r) - n I(r) \right], \tag{40}$$

and with the HC:

$$U(r) = w(r) + \frac{1}{\beta} \ln \left[1 + n I(r) \right] = -\frac{1}{\beta} \left[\ln \left(\frac{g(r)}{1 + n I(r)} \right) \right], \tag{41}$$

In both cases, $I(r)$ is the convolution integral defined as:

$$I(r) = \int \left[g(r') - 1 - n I(r') \right] \left[g(|\mathbf{r}' - \mathbf{r}|) - 1 \right] d^2 r', \tag{42}$$

which can be calculated numerically.

2.4.3 Anomalous effects

In order to understand the interactions in this kind of systems, we have to note that the standard theory of colloidal interactions, the DLVO theory, fails to explain several experimental observations. For example, an attractive interaction is observed between the particles when the electrostatic potential is obtained. This is a effect that has been previously observed in experiments on suspensions of confined equally-charged microspheres (Behrens & Grier (2001a;b); Grier & Han (2004); Han & Grier (2003); Larsen & Grier (1997)).

Grier and colleagues listed several experimental observations using suspensions of charged polystyrene particles with diameters around 0.65 microns at low ionic strength and strong spatial confinement. They note that such effects appear when a wall of glass or quartz is near the particles. Studying the $g(r)$ function and its relation to the interaction potential, given by expression 36, they showed the appearance of a minimum on the potential located at $z = 2.5$ microns of the wall and a distance between centres to be $r_{\min} = 3.5$ microns. This attraction cannot be a Van der Waals interaction, because for this type of particle and with separations greater than 0.1 micrometres, this force is less than $0.01\, k_B T$ (Pailthorpe & Russel (1982)), while this attractive interaction is about $0.7\, k_B T$.

The same group (Behrens & Grier (2001b)) extended this study using silica particle suspensions (silicon dioxide, SiO_2) of 1.58 microns in diameter, with a high density of 2.2 g/cm^3, using a cell of thickness $h = 200\,\mu$m. In this situation, even though the particles are deposited at a distance from the bottom edge of the particle to the bottom wall equal to $s = 0.11\,\mu$m, no minimum in the interaction energy between pairs appears, being the interaction purely repulsive, in the classical form of DLVO given by Eq.34. In that work, a methodology is also provided to estimate the Debye length of the system and the equivalent load Z^* through a study of the presence of negative charge quartz wall due to the dissociation of silanol groups in presence of water (Behrens & Grier (2001a)). However, Han & Grier (2003) observed the existence of a minimum in the potential when they use polystyrene particles of 0.65 micron and density close to water, 1.05 g/cm^3, with a separation between the walls of $h = 1.3$ microns. What is more, using silica particles from previous works, they observe a minimum separation between walls of $h = 9\,\mu$m.

The physical explanation of this effect is not clear (Grier & Han (2004)), being the main question how to explain the influence on the separation of the two walls in the confinement cell. However, some criticism has appeared about this results. For example, about the employment of a theoretical potential with a DLVO shape. An alternative is using a Sogami-Ise (SI) potential (Tata & Ise (1998)). Moreover, Tata & Ise (2000) contend that both the DLVO theory and the SI theory are not designed for situations in confinement, so interpreting the experimental data using either of these two theories may be wrong. Controversy on the use of a DLVO-type or SI potentials appears to be resolved considering that the two configurations represent physical exclusive situations (Schmitz et al. (2003)). In fact, simulations have been performed to explore the possibility of a potential hydrodynamic coupling with the bottom wall generated by the attraction between two particles (Dufresne et al. (2000); Squires & Brenner (2000)). However, the calculated hydrodynamic effects do not seem to explain the experimental minimum on the potential (Grier & Han (2004); Han & Grier (2003)). Other authors argue that this kind of studies should be more rigorous in the analysis of errors when extracting data from the images (Savin & Doyle (2005; 2007); Savin et al. (2007)) and other authors claim that the effect on the electrostatic potential may be an artefact (Baumgart et al. (2006)) that occurs because of a incorrect extraction of the position of the particles (Gyger et al. (2008)).

Polin et al. (2007) realized that some minimums in the electrostatic potential can be eliminated by measuring the error on the displacement of the particles. However, this is not a double implication and other experimental minimums in the potential remain there. In that work, the authors take into account all the proposed artefacts to date for their measurements, demonstrating that charged glass surfaces really induce attractions between charged colloidal spheres. Moreover, Tata et al. (2008) claim that their observations using confocal laser scanning of millions of charged colloidal particles establish the existence of an attractive behaviour in the electrostatic potential.
Moreover, other possible electrostatic variations in these systems may appear for several reasons. For instance, the emergence of a spontaneous macroscopic electric field in charged colloids (Rasa & Philipse (2004)). Moreover, according to several studies, changes in the fluid due to, for example, environmental pollution with atmospheric CO_2, can be relatively easy and are not negligible at low concentrations, being able to radically change the electrical properties on the fluid (Carrique & Ruiz-Reina (2009)). Thus, interactions related to colloidal stability can produce anomalous effects and significant changes in, for example, sedimentation kinetics (Buzzaccaro et al. (2008)) or sedimentation-diffusion profiles (Philipse & Koenderink (2003)). Then, these electrostatic effects can affect the dynamics of aggregation and influence the mobility of the particles and clusters.

3. Results

Our experimental system is formed by a MRF composed of colloidal dispersions of superparamagnetic micron-sized particles in water. These particles have a radius of 485 nm and a density of 1.85 g/cm^3, so they sediment to an equilibrium layer on the containing cell. They are composed by a polymer (PS) with nano-grains of magnetite dispersed into it, which provide their magnetic properties. The particles are also functionalized with carboxylic groups, so they have an electrical component, therefore, they repel each other, avoiding aggregation. This effect is improved by adding sodium dodecyl sulfate (SDS) in a concentration of 1 gr/l.
The containing cell consists on two quartz windows, one of them with a cavity of 100 μm. The cell with the suspension in it is located in an experimental setup that isolate thermically the suspension and allows to generate a uniform external magnetic field in the centre of the cell. The particles and aggregates are observed using video-microscopy (see details for this experimental setup on (Domínguez-García et al. (2007))). Images of the fluid are saved on the computer and then analysed for extracting the relevant data by using our own developed software (Domínguez-García & Rubio (2009)) based on *ImageJ* (*U. S. National Institutes of Health, Bethesda, Maryland, USA, http://rsb.info.nih.gov/ij/* (n.d.)). In Fig.3, we show an example of these microparticles and aggregates observed in our system.
The zeta potential of these particles is about -110 to -60 mV for a pH about 6 - 7. Therefore, the electrical content of the particles is relatively high and it is only neglected in comparison with the energy provided by the external magnetic field. However, the colloidal stability of these suspensions is not being controlled and it may have an effect on the dynamics of the clusters, specially when no magnetic field is applied. In any case, as we will see, even when a magnetic field is applied, it is observed a disagreement between theoretical aggregation times and experimental ones.

3.1 Control parameters

We have already defined some important parameters as the Péclet number, Eq.29, and the Reynolds number Eq.19. However, in our system we need to define some external parameters related with the concentration of particles and the intensity of the magnetic field. The concentration of volume of particles in the suspension, ϕ, is defined as the fraction of volume occupied by the spheres relative to the total volume of the suspension. In a quasi-2D video-microscopy system is useful to take into account the surface concentration ϕ_{2D}.
For measuring the influence of the magnetic interaction we used the λ parameter, defined as:

$$\lambda \equiv \frac{W_m}{k_B T} = \frac{\mu_s \mu_0 m^2}{16\pi a^3 k_B T} \tag{43}$$

as the ratio of $W_m = U_{ij}^d(r = 2a, \alpha = 0)$, i.e., the magnetic energy, and the thermal fluctuations $k_B T$. Here, μ_s is the relative magnetic permeability of the solvent, μ_0 the magnetic permeability of vacuum and m the magnetic moment. The parameters λ y ϕ_{2D} allow to define a couple of characteristic lengths. First, we define a distance R_1 for which the energy of dipolar interaction is equal to thermal fluctuations:

$$R_1 \equiv 2a\lambda^{1/3} \tag{44}$$

Finally, we define a mean distance between particles:

$$R_0 \equiv \sqrt{\pi} a \, \phi_{2D}^{-1/2} \tag{45}$$

The comparative between these two quantities allows to distinguish between different aggregation regimes. When, $R_1 < R_0$, the thermal fluctuations prevail over the magnetic interactions so diffusion is the main aggregation process. If $R_1 > R_0$, the aggregation of the particles occurs mainly because of the applied magnetic field.

3.2 Aggregation and disaggregation

Studies about the dynamics of the irreversible aggregation of clusters under unidirectional constant magnetic fields have used a collection of experimental systems. For example, electro-rheological fluids (Fraden et al. (1989)), magnetic holes (non-magnetic particles in a ferrofluid) (Cernak et al. (2004); Helgesen et al. (1990; 1988); Skjeltorp (1983)), and magneto-rheological fluids and magnetic particles (Bacri et al. (1993); Bossis et al. (1990); Cernak (1994); Cernak et al. (1991); Fermigier & Gast (1992); Melle et al. (2001); Promislow et al. (1994)).
These studies focus their efforts in calculating the kinetic exponent z obtaining different values ranging $z \sim 0.4 - 0.7$. The different methodologies employed can be the origin of these dispersed values. However, more recent studies (Domínguez-García et al. (2007); Martínez-Pedrero et al. (2007)) suggest that this value is approximately $z \sim 0.6 - 0.7$ in accordance with experimental values reported for aggregation of dielectric colloids $z \sim 0.6$ (Fraden et al. (1989)) and with recent simulations of aggregation of superparamagnetic particles (Andreu et al. (2011)). Regarding hydrodynamics interactions Miguel & Pastor-Satorras (1999) proposed and effective expression for explaining the dispersed value of the kinetic exponent based on logarithmic corrections in the diffusion coefficient (Eqs. 26 and 27):

$$S(t) \sim (t \ln [S(t)])^{\xi}, \tag{46}$$

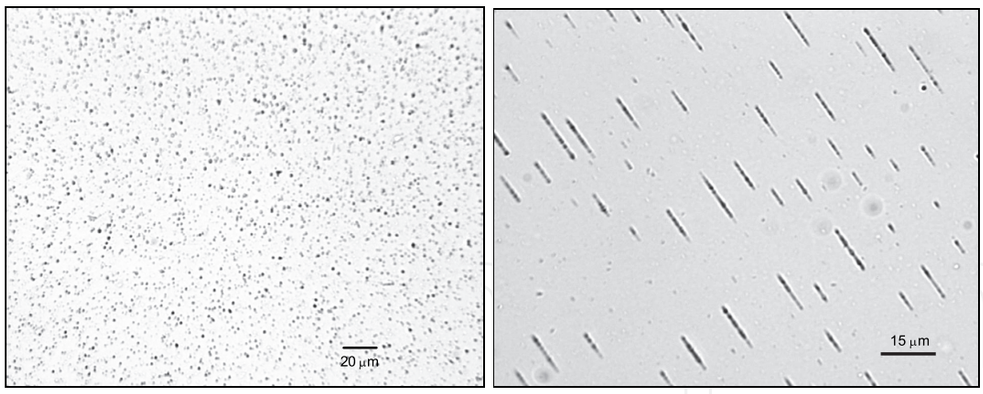

Fig. 3. Superparamagnetic microparticles observed when no external magnetic field is applied (Left) and when it is applied (Right).

where the exponent ξ is an exponent that depends on the dimensionality of the system, so if $d \geq 2$, $\xi = 1/2$. Using Monte Carlo simulations they obtain that $\xi \simeq 0.51$, and therefore that z is $z \simeq 0.61$.
In the case of our experiments, we have experimentally obtained that the z exponent in aggregation is contained in the range of $0.43 - 0.67$ (Domínguez-García et al. (2007)) with an average value of $z \sim 0.57 \pm 0.03$. These experimental values do not depend on the amplitude of the magnetic field nor on the concentration of particles, but they seem to depend on the ratio R_1/R_0, which is a sign of the more important regime of aggregation. The dependency on this ratio also appears when the morphology of the chains is studied (Domínguez-García, Melle & Rubio (2009); Domínguez-García & Rubio (2010)). Besides, the scaling behaviour given by Eq.7 is experimentally observed and checked. We have compared our experimental results with Brownian dynamics simulations based on a simple model which only included dipolar interaction between the particles, hard-sphere repulsion and Brownian diffusion, neglecting inertial terms and effects related with sedimentation or electrostatics. The results of these simulations agree with the theoretical prediction, whereas the experimental aggregation time, t_{ag}, appears to be much longer than expected (Cernak et al. (2004); Domínguez-García et al. (2007)), about three orders of magnitude of difference. The formation of dimers (two-particles aggregates) in the experiments lapses $t \sim 10^2$ seconds, but Brownian simulations show that this lapse of time is about $t \sim 0.1$ s. This last value can be easily obtained by assuming that the equation for the movement between two particles with dipolar magnetic interaction is:

$$M\ddot{r} + \gamma_0 \dot{r} + 3\mu\mu_0 m^2 r^{-4} \pi^{-1} = 0$$

where M is the mass of the particles. Because of Reynolds number (Eq.19) is very low, we neglect the inertial term on this equation. If the particles are separated a initial distance $d = R_0$ we can obtain that:

$$t_{\mathrm{ag}} \cong \frac{32\pi\gamma_0 a^5}{15\mu_s\mu_0 m^2} \phi_{2D}^{-5/2}$$

If we express this equation in function of the λ parameter 43 and of the diffusion coefficient given by the Stokes-Einstein equation 13:

$$t_{\mathrm{ag}} \cong \frac{2a^2}{15} \frac{1}{\lambda D} \phi_{2D}^{-5/2} \tag{47}$$

For example, the aggregation processes for $S(t)$ in the work of Promislow et al. (1994), show an aggregation time of 200 seconds. The paramagnetic particles used in that work have a diameter of 0.6 μm and a 27% of magnetite content. Using the Stokes-Einstein expression, $D = 0.86\,\mu\mathrm{m/s}^2$ is obtained, supposing that these particles do not sediment. Using $\phi = 0.0012$ and $\lambda = 8.6$, we can obtain that $t_{\mathrm{ag}} \sim 122$ seconds, in the order of their experimental result. In the case of our experiments, we obtain the same values using Eq.47 that using Brownian simulations.

These discrepancies may be related with hydrodynamic interactions which should affect the diffusion of the particles. From Eq.47, we see that some variation on the diffusion coefficient of the particles can modify the expected aggregation time for two particles. For testing that, we made some microrheology measurements using different types of isolated particles according to the theory of sedimentation and with the corrections on the values of the diffusion coefficient. The experimental values agree very well with the theoretical ones calculated from the expression 2.3.4 (Domínguez-García, Pastor, Melle & Rubio (2009)) but they imply a reduction on the diffusion coefficient a factor of three as a maximum, no being sufficient for explaining the discrepancy in the aggregation times.

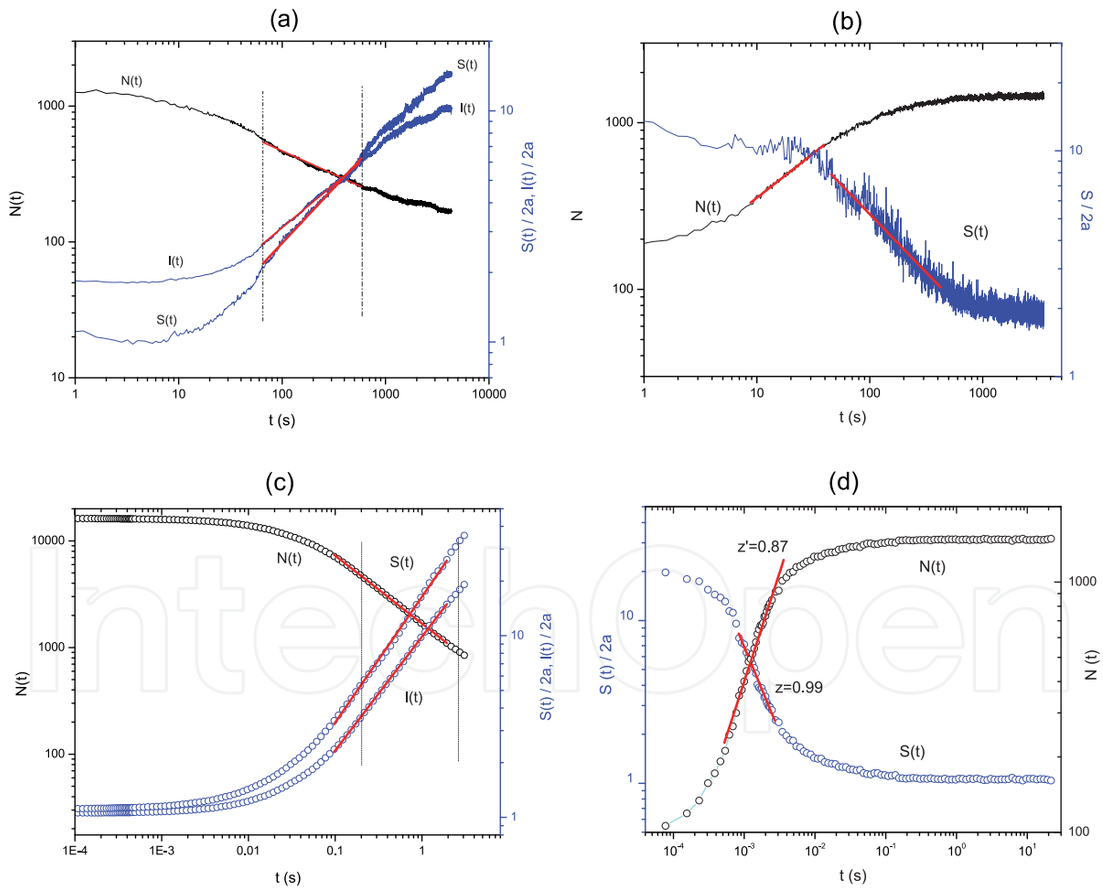

Fig. 4. Experiments of aggregation and disaggregation. The experimental process of aggregation (a) begins with $\lambda = 1718$, $\phi_{2D} = 0.088$ while disaggregation is shown in (b). Brownian dynamics simulations results with $\lambda = 100$, $\phi_{2D} = 0.03$ are shown for aggregation (c) and disaggregation (d). Data from Refs.(Domínguez-García et al. (2007; 2011))

For completing this study, we also have shown results of disaggregation, that is, the process that occurs when the external magnetic field is switched off and the clusters vanish. For this process we study the kinetics in the same way that in aggregation, by searching power laws behaviours and calculating the kinetic exponents z and z' (Domínguez-García et al. (2011)). We have also developed Brownian dynamics simulations to be compared with the experiments. The Fig.4 summarizes some of our results in aggregation and disaggregation. The experimental kinetic exponents during disaggregation range from $z = 0.44$ to 1.12 and $z' = 0.27$ to 0.67, while simulations give very regular values, with z and $z' \sim 1$. Then, the kinetic exponents do not agree, being also the process of disaggregation much faster in simulations. From these results, we conclude that remarkable differences exist between a simple theoretical model and the interactions in our experimental setup, differences that are specially important when the influence of the applied magnetic field is removed.
In all these experiments some data has been collected before any external field is applied. That allows us to study the microstructure of the suspensions by calculating the electrostatics potential using the methods previously explained. The inversion of the O-Z equation reveals an attractive well in the potential with a value in its minimum in the order of $-0.2\,k_BT$, similar to other observations of attractive interactions of sedimented particles in confinement situations. Moreover, these values of the minimum in the potential seems to depend of the concentration of particles (Domínguez-García, Pastor, Melle & Rubio (2009)), something which is expected, if it is related in some way with the electrical charge contained in the suspension.

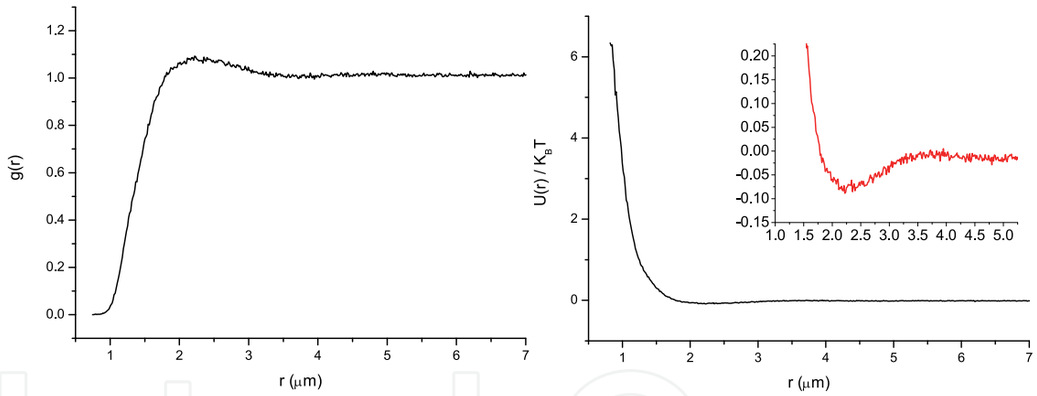

Fig. 5. Left: $g(r)$ function, Right: Electrostatic potential calculated by inverting the O-Z equation (all the approximations give the same result) Inset: a detail for $U(r)$ in the region of the minimum. Number density $n = 0.0009$

As a confirmation of these results, we show here a calculation of the electrostatic potential using a long set of images of charged superparamagnetic microparticles spreading in the experimental system described above. We have obtained images of the suspension during more than an hour, with a temporal lapse between images of 0.3 seconds. This data allow us to produce a very defined graph for the pair correlation function, showed in the Fig.5. In the right side of the Fig.5, we plot the electrostatic potential and in its inset we can see that the minimum has a value of about $-0.1\,k_BT$, confirming the previous results obtained in this experimental setup.
However, this result may be an effect of an imagining artefact. About that question, some of the studies which use particle tracking only apply some filters to the images for detecting brightness points and then extracting the position of the particles. Our image analysis

software (Domínguez-García & Rubio (2009)) employs open-sourced algorithms for detecting the centres of mass of the particles by detecting the borders of each object and then obtaining its geometrical properties. As an example, we have tried to evaluate how this border detection can have an influence on the result of the electrostatic potential. A measured apparent displacement $\Delta(r) = r' - r$ should affect to the radial distribution function in the following form: $g(r) = g'(r + \Delta(r))(1 + d\Delta(r)/dr)$ (Polin et al. (2007)). From that expression, the variation in the electrostatic potential is:

$$\beta U'(r) - \beta U(r) \cong -\beta \frac{dU(r)}{dr} \Delta(r) + \frac{d\Delta(r)}{dr} \tag{48}$$

For obtaining $\Delta(r)$ we have extracted a typical particle image and we have composed some set of images which consist on separating the two particles a known distance (r) in pixels. Next, we apply our methods of image analysis for obtaining the position of those particles and calculate the distances (r'). Then, the apparent displacement, $\Delta(r) = r' - r$, is observed to grow when the particles are very near. In Fig.6, we display the results of our calculations on the possible artefact in the analysis of the position of the particles by image binarization and binary watershed, a method for automatically separating particles that are in contact. The figure reveals that the correction on the electrostatic potential for this cause is basically negligible, because the correction in the potential is zero for distances $r > 1.2$ μm. In the inset of the figure we can see some of the images we have employed for this calculation, showing the detected border of the particles among the images themselves.

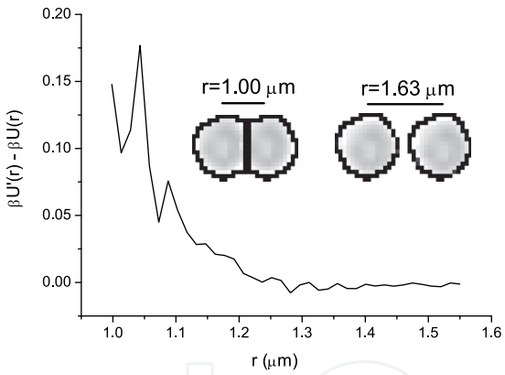

Fig. 6. Estimation of a possible artefact in the analysis of the position of the particles. In the inset we have included some examples of the images used for this calculation.

In any case, the possibility of an artifact can be the cause of these observations in the electrostatic potential cannot be descarted. However, the direct or indirect presence and influence of these attractive wells has been detected in many other situations in these experiments. For example, the attractive interaction disappears when we added a salt, in our case KCl, to the suspensions, confirming the electrostatic nature of the phenomena (Domínguez-García, Pastor, Melle & Rubio (2009)). In disaggregation it is observed how the particles move inside the chains without leaving them (Domínguez-García et al. (2011)). The lapse of time that the particles are in this situation depends on the initial morphology of the aggregates, something which has been observed to depend on the ratio R_1/R_0 (Domínguez-García, Melle & Rubio (2009); Domínguez-García & Rubio (2010)). Then, this effective lapse of time depends of how many particles are located near the other in a short distance. In that situation, the attractive interaction should play a role in disaggregation, as it

seems to be. Indeed, this "detaining" effect of the particles inside the clusters is not observed in experiments with added salt.
What is more, we have also observed that the kinetic exponents during aggregation are different and slower if we add salt to the suspension (Domínguez-García et al. (2011)). This last effect may be related with an unexpected interaction of the particles with the charged quartz bottom wall by means of a a spontaneous macroscopic electric field. When the particles and clusters have no electrical component, they should be highly sedimented at the bottom of the quartz cell and the resistance to their the movement should be increased (Kutthe (2003)), generating that the kinetic exponents reduce their value.

4. Conclusions

In this chapter, we have reviewed the main interactions, with focus on hydrodynamics and from a experimental point of view, that can be important in a confined colloidal system at low concentration of microparticles. We have used charged superparamagnetic microparticles dispersed in water in low-confinement conditions by means of a glass cell for the study of irreversible field-induced aggregation and disaggregation, as well as the microstructure of the suspension. Regarding aggregation characteristic times and basic behaviour on the disaggregation of the particles, we have observed significant discrepancies between the experimental results and the theory. Morover, anomalous effects in the electrostatic behaviour have been observed, showing that, in this kind of systems, the electro-hydrodynamics interactions are not well understood at present and deserve more theoretical and experimental investigations.

5. Acknowledgements

We wish to acknowledge Sonia Melle and J.M. Pastor for all the work done, J.M M. González, J.M. Palomares and F. Pigazo (ICMM) for the VSM magnetometry measurements and J.C. Gómez-Sáez for her proofreading of the English texts. This research has been partially supported by M.E.C. under Project No. FIS2006-12281-C02-02, M.C.I under FIS2009-14008-C02-02, C.A.M under S/0505/MAT/0227 and UNED by 2010V/PUNED/0010.

6. References

Andreu, J. S., Camacho, J. & Faraudo, J. (2011). Aggregation of superparamagnetic colloids in magnetic fields: the quest for the equilibrium state, 7: 2336.

Bacri, J. C., Djerfi, K. & Neveu, S. (1993). Ferrofluid viscometer - transient magnetic birrefrigence in crossed fields, *J. Mag. Mat.* 123 (1-2): 67–73.

Baumgart, J., Arauz-Lara, J. L. & Bechinger, C. (2006). Like-charge attraction in confinement: myth or truth?, *Soft Matter* 2: 631–635.

Behrens, S. H. & Grier, D. G. (2001a). The charge of glass and silica surfaces, *J. Chem. Phys.* 115: 6716–6721.

Behrens, S. H. & Grier, D. G. (2001b). Pair interaction of charged colloidal spheres near a charged wall, *Phys. Rev. E* 64: 050401(R).

Bensech, T. & Yiacoumi, S. (2003). Brownian motion in confinement., *Phys. Rev. E* 68: 021401.

Bossis, G., Mathis, C., Minouni, Z. & Paparoditis, C. (1990). Magnetoviscosity of micronic particles, *Europhys. Lett.* 11: 133.

Brenner, H. (1961). The slow motion of a sphere through a viscous fluid towards a plane surface., *Phys. Rev. E* 68: 021401.

Buzzaccaro, S., Tripodi, A., Rusconi, R., Vigolo, D. & Piazza, R. (2008). Kinetics of sedimentation in colloidal suspensions, *J. Phys. Condens. Matter* (20): 494219.

Carrique, F. & Ruiz-Reina, E. (2009). Effects of water dissociation and co2 contamination on the electrophoretic mobility of a spherical particles in aqueous salt-free concentrated suspensions, *J. Phys. Chem. B* (113): 8613–8625.

Cernak, J. (1994). Aggregation of needle-like macro-clusters in thin-layers of magnetic fluid, *J. Magn. Magn. Mater.* 132: 258.

Cernak, J., Helgesen, G. & Skjeltorp, A. T. (2004). Aggregation dynamics of nonmagnetic particles in a ferrofluid, *Phys. Rev. E* 70 (3): 031504 Part 1.

Cernak, J., Macko, P. & Kasparkova, M. (1991). Aggregation and growth-processes in thin-films of magnetic fluid, *J. Phys. D: Appl. Phys.* 24: 1609.

Chen, H. & Ma, H. (2006). The density profile of hard sphere liquid system under gravity., *J. Chem. Phys.* 125: 024510.

Crocker, J. C. (1997). Measurement of the hydrodynamic corrections of the Brownian motion of two colloidal spheres., *J. Chem. Phys.* 106: 2837–2840.

Crocker, J. C. & Grier, D. G. (1996). Methods of digital video microscopy for colloidal studies, *J. Colloid Interface Sci.* 179: 298–310.

Crocker, J. C., Valentine, M. T., Weeks, E. R., Gisler, T., Kaplan, P. D., Yodh, A. G. & Weitz, D. A. (2000). Two-point microrheology of inhomogeneous soft materials, *Phys. Rev. Lett.* 85: 888–891.

Derjaguin, B. V. & Landau, L. (1941). Theory of the stability of strongly charged lyophobic sols and of the adhesion of strongly charged particles in solution of electrolytes., *Acta Physicochim. URSS* 14: 633.

Doi, M. & Edwards, S. (1986). *The Theory of Polymer Dynamics.*, Clarendon Press, Oxford.

Domínguez-García, P., Melle, S., Pastor, J. M. & Rubio, M. A. (2007). Scaling in the aggregation dynamics of a magneto-rheological fluid., *Phys. Rev. E* 76: 051403.

Domínguez-García, P., Melle, S. & Rubio, M. A. (2009). Morphology of anisotropic chains in a magneto-rheological fluid during aggregation and disaggregation processes., *J. Colloid Interface Sci.* 333: 221–229.

Domínguez-García, P., Pastor, J. M., Melle, S. & Rubio, M. A. (2009). Electrostatic and hydrodynamics effects in a sedimented magneto-rheological suspension, *Phys. Rev. E* 80: 0214095.

Domínguez-García, P., Pastor, J. M. & Rubio, M. A. (2011). Aggregation and disaggregation dynamics of sedimented and charged superparamagnetic microparticles in water suspension, *Europhys. J. E. Soft. Matter.* 34: 36.

Domínguez-García, P. & Rubio, M. A. (2009). Jchainsanalyser: an imagej-based stand-alone application for the study of magneto-rheological fluids., *Comput. Phys. Commun.* 80: 1956–1960.

Domínguez-García, P. & Rubio, M. A. (2010). Three-dimensional morphology of field-induced chain-like aggregates of superparamagnetic micro-particles, *Colloids Surf., A* 358: 21–27.

Dufresne, E. R., Altman, D. & Grier, D. G. (2001). Brownian dynamics of a sphere between parallel walls, *Europhys. Lett.* 53: 264–270.

Dufresne, E. R., Squires, T. M., Brenner, M. P. & Grier, D. G. (2000). Hydrodynamic coupling of two brownian spheres to a planar surface, *Phys. Rev. Lett.* 85(15): 3317–3320.

Egatz-Gómez, A., Melle, S., García, A. A., Lindsay, S. A., Márquez, M., Domínguez-García, P., Rubio, M. A., Picraux, S. T., Taraci, J. L., Clement, T., Yang, D., Hayes, M. A. & Gust, D. (2006). Discrete magnetic microfluidics, *Appl. Phys. Lett.* 89(3)(034106).

Faucheux, L. P. & Libchaber, A. J. (1994). Confined brownian motion, *Phys. Rev. E* 49: 5158.

Fermigier, M. & Gast, A. P. (1992). Structure evolution in a paramagnetic latex suspension, *J. Colloid Interface Sci.* 154: 522.

Fraden, S., Hurd, A. J. & Meyer, R. B. (1989). Electric-field-induced association of colloidal particles, *Phys. Rev. Lett.* 63 (21): 2373–2376.

Furst, E. M. (2005). Applications of laser tweezers in complex fluid rheology., *Curr. Opin. Colloid Interface Sci.* 10: 79–86.

Furst, E. M. & Gast, A. P. (2000). Micromechanics of magnetorheological suspensions, *Phys. Rev. E* 61: 6732.

González, A. E., Odriozola, G. & Leone, R. (2004). Colloidal aggregation with sedimentation: concentration effects., *Europhys. J. E. Soft. Matter.* 13: 165–178.

Grier, D. G. (2003). A revolution in optical manipulation., *Nature* 424: 810–815.

Grier, D. G. & Han, Y. (2004). Anomalous interactions in confined charge-stabilized colloid, *J. Phys. Condens. Matter* 16: 4145–4157.

Gyger, M., Rückerl, F., Käs, J. A. & Ruiz-García, J. (2008). Errors in two particle tracking at close distances, *J. Colloid Interface Sci.* 326: 382–386.

Halsey, T. C. & Toor, W. (1990). Structure of electrorheological fluids, *Phys. Rev. Lett.* 65: 2820.

Han, Y. & Grier, D. G. (2003). Confinement-induced colloidal attractions in equilibrium, *Phys. Rev. Lett.* 91(3): 038302.

Helgesen, G., Pieranski, P. & Skjeltorp, A. T. (1990). Nonlinear phenomena in systems of magnetic holes, *Phys. Rev. Lett.* 64 (12): 1425–1428.

Helgesen, G., Skjeltorp, A. T., Mors, P. M., Botet, R. & Jullien, R. (1988). Aggregation of magnetic microspheres: Experiments and simulations, *Phys. Rev. Lett.* 61(15): 1736–1739.

Hernández-Ortiz, J. P., Ma, H., de Pablo, J. J. & Graham, M. D. (2006). Cross-stream-line migration in confined flowing polymer solutions: Theory and simulation., *Phys. Fluids* 18: 123101.

Jendrejack, R. M., Schwartz, D. C., Graham, M. D. & de Pablo., J. J. (2003). Effect of confinmeent on DNA dynamics in microfluidic devices., *J. Chem. Phys.* 119(2): 1165–1173.

Keller, M., Schilling, J. & Sackmann, E. (2001). Oscillatory magnetic bead rheometer for complex fluid microrheometry, *Rev. Sci. Instr.* 72(9): 3626.

Kerr, R. A. (1990). *Science* 247: 050401.

Kolb, M., Botet, R. & Jullien, R. (1983). Scaling of kinetically growing clusters, *Phys. Rev. Lett.* 51: 1121–1126.

Komeili, A. (2007). Molecular mechanisms of magnetosome formation., *Annu. Rev. Biochem.* 76: 351–356.

Koppel, D. E. (1972). Analysis of macromolecular polydispersity in intensity correlation spectroscopy: The method of cumulants., *J. Chem. Phys.* 57(11): 4814–4820.

Kutthe, R. (2003). Stokesian dynamics of nonspherical particles, chains, and aggregates., *J. Chem. Phys.* 119(17): 9280–9294.

Larsen, A. E. & Grier, D. G. (1997). Like-charge attraction in metastable colloidal crystallites, *Nature* 385(16): 230–233.

Larson, R. G. (1999). *The Structure and Rheology of Complex Fluids*, Oxford University Press, NewYork.

Lian, Z. & Ma, H. (2008). Electrostatic interaction between two nonuniformly charged colloid particles confined in a long charged cylinder wall., *J. Phys. Condens. Matter* 20: 035109.
Lin, B., Yu, J. & Rice, S. A. (2000). Direct measurements of constrained Brownian motion of an isolated sphere between two walls., *Phys. Rev. E* 62 (3): 3909–3919.
Lin, M. Y., Lindsay, H. M., Weitz, D. A., Ball, R. C., Klein, R. & Meakin, P. (1989). Universality in colloid aggregation, *Nature* 339(1): 360–362.
Liron, N. & Mochon, S. (1976). Stokes flow for a stokeslet between two parallel flat plates., *J. Eng. Math.* 10 (4): 287–303.
Lord Corporation, http://www.lord.com/ (n.d.).
Martin, J. E. & Anderson, R. A. (1996). Chain model of electrorheology, *J. Chem. Phys.* 104: 4814.
Martin, J. E., Odinek, J. & Halsey, T. C. (1992). Evolution of structure in a quiescent electrorheological fluid, *Phys. Rev. Lett.* 69 (10): 1524–1527.
Martínez-Pedrero, F., Tirado-Miranda, M., Schmitt, A. & Callejas-Fernández, J. (2007). Formation of magnetic filaments: A kinetic study., *Phys. Rev. E* 76: 011405.
Mason, T. G. (2000). Estimating the viscoelastic moduli of complex fluid using the generalized stokes-einstein equation, *Rheol. Acta* 39: 371–378.
Mason, T. G. & Weitz, D. A. (1995). Optical measurements of frequency-dependent linear viscoelastic moduli of complex fluids, *Phys. Rev. Lett.* 74: 1250 – 1253.
Meakin, P. (1983). Formation of fractal clusters and networks by irreversible diffusion-limited aggregation, *Phys. Rev. Lett.* 51: 1119–1122.
Melle, S. (2002). *Estudio de la dinámica de suspensiones magneto-reológicas sometidas a campos externos mediante el uso de técnicas ópticas. Procesos de agregación, formación de estructuras y su evolución espacio-temporal.*, PhD thesis, Universidad Nacional de Educación a Distancia.
Melle, S., Rubio, M. A. & Fuller, G. G. (2001). Time scaling regimes in aggregation of magnetic dipolar particles: scattering dichroism results., *Phys. Rev. Lett.* 87(11): 115501.
Miguel, M. C. & Pastor-Satorras, R. (1999). Kinetic growth of field-oriented chains in dipolar colloidal solutions, *Phys. Rev. E* 59 (1): 826–834.
Miyazima, S., Meakin, P. & Family, F. (1987). Aggregation of oriented anisotropic particles, *Phys. Rev. A* 36 (3): 1421–1427.
*N*akano, M. & Koyama, K. (eds) (1998). *Proceedings of the 6th International Conferences on ER and MR fluids and their applications*, World Scientific, Singapore.
Odriozola, G., Jiménez-Ángeles, F. & Lozada-Cassou, M. (2006). Effect of confinement on the interaction between two like-charged rods., *Phys. Rev. Lett.* 97: 018102.
Otterstedt, J. & Brandreth., D. A. (1998). *Small Particles Technology.*, Springer.
Paddinga, J. T. & Briels, W. J. (2010). Translational and rotational friction on a colloidal rod near a wall, *J. Chem. Phys.* 132: 054511.
Pailthorpe, B. A. & Russel, W. B. (1982). The retarded van der Waals interaction between spheres, *J. Colloid Interface Sci.* 89(2): 563–566.
Philipse, A. P. & Koenderink, G. H. (2003). Sedimentation-diffusion profiles and layered sedimentation of charged colloids at low ionic strength, *Adv. Colloid Interface Sci.* 100–102: 613–639.
Polin, M., Grier, D. G. & Han, Y. (2007). Colloidal electrostatic interactions near a conducting surface., *Phys. Rev. E* 76: 041406.
Promislow, J., Gast, A. P. & Fermigier, M. (1994). Aggregation kinetics of paramagnetic colloidal particles, *J. Chem. Phys.* 102(13): 5492–5498.
Rabinow, J. (1948). The magnetic fluid clutch, *AIEE Trans.* 67: 1308.

Rasa, M. & Philipse, A. P. (2004). Evidence for a macroscopic electric field in the sedimentation profiles of charged colloids, *Nature* 429(24): 857–860.

Reiner, E. S. & Radke, C. J. (1993). Double layer interactions between charge-regulated colloidal surfaces: Pair potentials for spherical particles bearing ionogenic surfaces groups., *Adv. Colloid Interface Sci.* 47: 59–147.

Russel, W. B., Saville, D. A. & Schowalter, W. R. (1989). *Colloidal Dispersions.*, Cambridge University Press.

Savin, T. & Doyle, P. S. (2005). Static and dynamic error in particle tracking microrheology, *Biophysical Journal* 88: 623–638.

Savin, T. & Doyle, P. S. (2007). Statistical and sampling issues when using multiple particle tracking, *Phys. Rev. E* 76: 021501.

Savin, T., Spicer, P. T. & Doyle, P. S. (2007). A rational approach to noise characterization in video microscopy particle tracking, *Phys. Rev. E* 76: 021501.

Schmidt, M., Dijkstra, M. & Hansen, J. P. (2004). Competition between sedimentation and phase coexistence of colloidal dispersions under gravity, *J. Phys. Condens. Matter* 16: S4185–S4194.

Schmitz, K. S., Bhuiyan, L. B. & Mukherjee, A. K. (2003). On the grier-crocker/tata-ise controversy on the macroion-macroion pair potential in a salt-free colloidal suspension, *Langmuir* 19: 7160–7163.

Science. (1999). Complex systems., *Science* 284(5411): 1–212.

Shen, L., Stachowiak, A., Fateen, S. E. K., Laibinis, P. E. & Hatton, T. A. (2001). Structure of alkanoic acid stabilized magnetic fluids. A small-angle neutron and light scattering analysis, *Langmuir* 17: 288.

Skjeltorp, A. T. (1983). One-dimensional and two-dimensional crystallization of magnetic holes, *Phys. Rev. Lett.* 51 (25): 2306–2309.

Smirnov, P., Gazeau, F., Lewin, M., Bacri, J. C., Siauve, N., Vayssettes, C., Cuenod, C. A. & Clement, O. (2004). In vivo cellular imaging of magnetically labeled hybridomas in the spleen with a 1.5-t clinical mri system, *Magn. Reson. Medi.* 52: 73–79.

Squires, T. M. & Brenner, M. P. (2000). Like-charge attraction and hydrodynamic interaction, *Phys. Rev. Lett.* 85(23): 4976–4979.

Tao, R. (ed.) (2000). *Proceedings of the 7th International Conferences on ER and MR fluids*, World Scientific, Singapore.

Tata, B. V. R. & Ise, N. (1998). Monte carlo study of structural ordering in charged colloids using a long-range attractive interaction, *Phys. Rev. E* 58(2): 2237–2246.

Tata, B. V. R. & Ise, N. (2000). Reply to "comment on 'monte carlo study of structural ordering in charged colloids using a long-range attractive interaction' ", *Phys. Rev. E* 61(1): 983–985.

Tata, B. V. R., Mohanty, P. S. & Valsakumar, M. C. (2008). Bound pairs: Direct evidence for long-range attraction between like-charged colloids, *Solid State Communications* 147: 360–365.

Tirado, M. M. & García, J. (1979). Translational friction coeffcients of rigid, symmetric top macromolecules. Application to circular cylinders., *J. Chem. Phys.* 71: 2581.

Tirado, M. M. & García, J. (1980). Rotational dynamics of rigid symmetric top macromolecules. Application to circular cylinders., *J. Chem. Phys.* 73: 1986.

Tirado-Miranda, M. (2001). *Agregación de Sistemas Coloidales Modificados Superficialmente.*, PhD thesis, Universidad de Granada.

U. S. National Institutes of Health, Bethesda, Maryland, USA, http://rsb.info.nih.gov/ij/ (n.d.).

Verdier, C. (2003). Rheological properties of living materials., *J. Theor. Medic.* 5: 67–91.
Verwey, E. J. W. & Overbeek, J. T. G. (1948). *Theory of the Stability of Lyophobic Colloids.*, Elsevier, Amsterdam.
Vicsek, T. (1992). *Fractal Growth Phenomena*, 2 edn, World Scientific, Singapore.
Vicsek, T. & Family, F. (1984). Dynamic scaling for aggregation of clusters, *Phys. Rev. Lett.* 52,19: 1669–1672.
von Smoluchowski, M. (1917). *Z. Phys. Chem., Stoechiom. Vertwanddtschaftsl* 92: 129.
Vuppu, A. K., García, A. A., Hayes, M. A., Booksh, K., Phelan, P. E., Calhoun, R. & Saha, S. K. (2004). Phase sensitive enhancement for biochemical detection using rotating paramagnetic particle chains, *J. Appl. Phys.* 96: 6831–6838.
Waigh, T. A. (2005). Microrheology of complex fluids, *Rep. Prog. Phys.* 68: 685–742.
Wilhelm, C., Browaeys, J., Ponton, A. & Bacri, J. C. (2003). Rotational magnetic particles microrheology: The maxwellian case, *Phys. Rev. E* 67: 011504.
Wilhelm, C., Gazeau, F. & Bacri, J. C. (2003). Rotational magnetic endosome microrheology: Viscoelastic architecture inside living cells, *Phys. Rev. E* 67: 061908.
Wilhelm, C., Gazeau, F. & Bacri, J. C. (2005). Magnetic micromanipulation in the living cell, *Europhys. news* 3: 89.
Witten, T. A. & Sander, L. M. (1981). Diffusion-limited aggregation, a kinetic critical phenomenon, *Phys. Rev. Lett.* 47: 1400–1403.

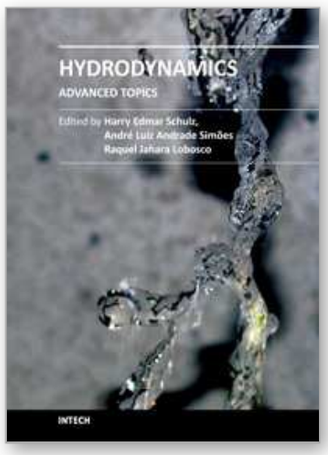

Hydrodynamics - Advanced Topics
Edited by Prof. Harry Schulz

ISBN 978-953-307-596-9
Hard cover, 442 pages
Publisher InTech
Published online 22, December, 2011
Published in print edition December, 2011

The phenomena related to the flow of fluids are generally complex, and difficult to quantify. New approaches - considering points of view still not explored - may introduce useful tools in the study of Hydrodynamics and the related transport phenomena. The details of the flows and the properties of the fluids must be considered on a very small scale perspective. Consequently, new concepts and tools are generated to better describe the fluids and their properties. This volume presents conclusions about advanced topics of calculated and observed flows. It contains eighteen chapters, organized in five sections: 1) Mathematical Models in Fluid Mechanics, 2) Biological Applications and Biohydrodynamics, 3) Detailed Experimental Analyses of Fluids and Flows, 4) Radiation-, Electro-, Magnetohydrodynamics, and Magnetorheology, 5) Special Topics on Simulations and Experimental Data. These chapters present new points of view about methods and tools used in Hydrodynamics.

How to reference
In order to correctly reference this scholarly work, feel free to copy and paste the following:

P. Domînguez-Garcîa and M.A. Rubio (2011). Hydrodynamics on Charged Superparamagnetic Microparticles in Water Suspension: Effects of Low-Confinement Conditions and Electrostatics Interactions, Hydrodynamics - Advanced Topics, Prof. Harry Schulz (Ed.), ISBN: 978-953-307-596-9, InTech, Available from: http://www.intechopen.com/books/hydrodynamics-advanced-topics/hydrodynamics-on-charged-superparamagnetic-microparticles-in-water-suspension-effects-of-low-confine

INTECH
open science | open minds

InTech Europe
University Campus STeP Ri
Slavka Krautzeka 83/A
51000 Rijeka, Croatia
Phone: +385 (51) 770 447
Fax: +385 (51) 686 166
www.intechopen.com

InTech China
Unit 405, Office Block, Hotel Equatorial Shanghai
No.65, Yan An Road (West), Shanghai, 200040, China
中国上海市延安西路65号上海国际贵都大饭店办公楼405单元
Phone: +86-21-62489820
Fax: +86-21-62489821

IntechOpen